High-temperature properties of the Sr_2FeMoO_6 double perovskite: Electrical resistivity, magnetic susceptibility, and ESR

D. Niebieskikwiat,[1] R. D. Sánchez,[1,2] A. Caneiro,[1] L. Morales,[1,2] M. Vásquez-Mansilla,[1] F. Rivadulla,[3] and L. E. Hueso[4]
[1]*Comisión Nacional de Energía Atómica-Centro Atómico Bariloche and Instituto Balseiro, 8400 Bariloche, Argentina*
[2] *CONICET, Argentina*
[3]*Department of Physical Chemistry, University of Santiago de Compostela, 15706 Santiago de Compostela, Spain*
[4]*Department of Applied Physics, University of Santiago de Compostela, 15706 Santiago de Compostela, Spain*
(Received 29 December 1999)

In this work we present electrical resistivity, magnetic susceptibility, and electron spin resonance data at high temperature of the Sr_2FeMoO_6 double perovskite. We found between 300 K and 900 K two metal-insulator transition temperatures at $T_c \approx 405$ K and ≈ 590 K respectively. Below the first transition, the material is metallic and magnetically ordered. Above 590 K, ρ shows a metallic behavior again, while in the range $405\,\mathrm{K} \leqslant T \leqslant 590\,\mathrm{K}$ we observed a weak localization. The magnetic susceptibility can be described taking into account localized and itinerant electrons. The paramagnetic resonance of Fe^{3+} ions with $g = 2.009(5)$ can be studied in temperature. Above T_c the linewidth data present similar behavior to that of manganese perovskites, with a relaxation mechanism related to spin-spin interactions. The intensity of the resonance line decreases with T faster than a Curie law expected, due to a reduction in the number of localized spins of the Fe^{3+} ions. At high temperatures ($T \geqslant 520$ K) we observe a second paramagnetic resonance line with $g = 1.995(1)$ associated with a small amount of Mo^{5+} ions.

I. INTRODUCTION

Manganese oxides in the perovskite structure have recently attracted a great interest of solid state scientists because of their particular structural, magnetic, and electronic properties. The recent discovery of huge negative magnetoresistance near the Curie temperature, called colossal magnetoresistance (CMR),[1,2] in lanthanum manganite doped with cations such as M^{2+} ($M = \mathrm{Ca, Sr, Ba}$) has created renewed interest in these compounds and has shown promise regarding potential applications.

More recently, in this context, polycrystalline samples of an ordered double perovskite Sr_2FeMoO_6 have been reported as a promising material for practical devices due to the presence of magnetoresistance at room temperature.[3] After that, epitaxial films of this compound in a narrow window of temperature and oxygen pressure have been made.[4] A band calculation[3] predicts half metallic band structure where the conduction electrons are highly spin polarized even at room temperature ($T \leqslant T_C$). In these cases, the magnetoresistance has been associated with electron tunneling[5] through an insulating barrier formed at the grain boundaries. Similar behavior has been reported in the parent compounds with Re.[6]

From pioneer studies[7,8] in the A_2FeMoO_6 ($A = \mathrm{Ca, Sr, Ba}$) series, it is known that the Sr_2FeMoO_6 compound has the maximum Curie temperature. Early magnetic,[9] Mössbauer, and neutron diffraction[10] experiments were made showing that Sr_2FeMoO_6 is ferrimagnetic with Fe^{3+} and Mo^{5+} electronic configuration. Alternatively to this traditional picture of magnetic order, a recent work[11] proposes the Fe^{2+} and Mo^{6+} configuration for this compound and other mechanisms to explain the magnetoresistance at room temperature.

In this work we present a systematic study of the magnetic, electron spin resonance (ESR) and transport properties of Sr_2FeMoO_6 at high temperature.

II. EXPERIMENT

A powdered sample of Sr_2FeMoO_6 was prepared by the solid-state reaction technique. Raw materials were Fe_2O_3, CO_3Sr, and metallic MoO_3 (99.99%). The raw materials were mixed and heated at 950°C in a 10% H_2/Ar atmosphere. A final heat treatment at 1150°C under high vacuum (a pressure of approximately 10^{-6} Torr) was performed for 12 h.

Powder x-ray diffraction (XRD) data were recorded on a Phillips PW 1700 diffractometer using Cu $K\alpha$ radiation and a graphite monochromator. X-ray data at room temperature were refined by the Rietveld method with the FULLPROF program.[12] Our refinement of the x-ray diffraction was made on the basis of the tetragonal $I4/m$ space group. The obtained lattice parameters were $a = b = 5.5770(2)$ Å and $c = 7.9053(3)$ Å. No secondary phases were detected neither by x-ray nor by scanning electron microscope (SEM) observations.

High-temperature electrical resistivity (ρ) measurements were carried out by a standard four-probe ac technique with a lock-in amplifier on a dense sample under a vacuum of approximately 10^{-6} Torr, similar to that used to prepare the sample.

The magnetization (M) data were measured in a commercial Quantum Design superconducting quantum interference device (SQUID) magnetometer in the $5\,\mathrm{K} \leqslant T \leqslant 300\,\mathrm{K}$ temperature range. From room temperature to 600 K a homemade Faraday balance was used. Approximately 10 mg of sample were placed in a sealed quartz tube of 3 mm in diameter filled with 10% H_2/Ar gas.

In both magnetometers, the M vs T curves were obtained

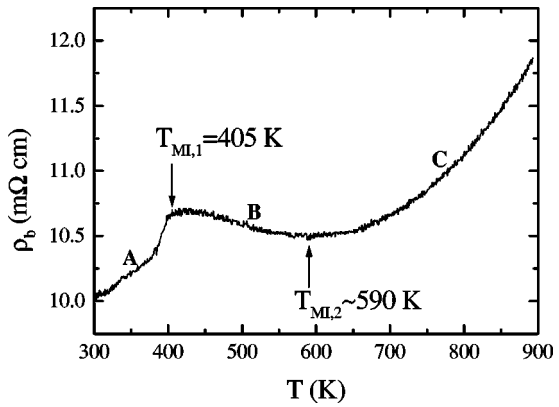

FIG. 1. Bulk electrical resistivity as a function of temperature of Sr_2FeMoO_6. The arrows indicate the two metal-insulator transitions of the compound that define the sequence metal (A), semiconducting (B), and metal (C) regions. The data were obtained at a pressure of 10^{-6} Torr.

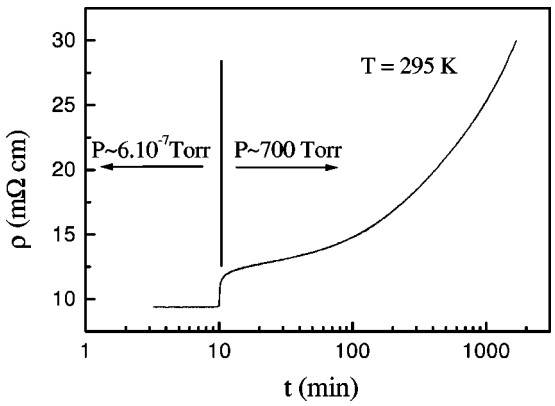

FIG. 2. Time evolution of the electrical resistivity at room temperature. The step in ρ occurs when the vacuum is broken.

applying a magnetic field (H) of 5 kG and the magnetic susceptibility (χ) was computed as the ratio M/H. Hysteresis loops were taken between -50 kG and 50 kG in the temperature range 5–300 K. For this perovskite, the diamagnetic contribution of the atomic cores was estimated to be -120×10^{-6} emu/mol and it was subtracted from the experimental data.

The ESR experiments were performed at 9.5 GHz using a Bruker ESP-300 spectrometer from 300 K to 600 K.

III. RESULTS

A. Electrical resistivity

The bulk electrical resistivity ($\rho\sim\rho_b\approx0.01$ Ω cm) data were obtained after heating the sample under a vacuum of 10^{-6} Torr from room temperature to 900 K. During this heating process the resistivity showed a strong semiconducting behavior, with an initial resistivity at room temperature of ≈100 mΩ cm and reaching ≈13 mΩ cm at 900 K. At this temperature an evolution of ρ with time was observed, which stopped after ≈4 h with a resistivity value of ≈12 mΩ cm. We assume that this change is associated with a change of the oxygen content at the grain boundaries. When this evolution stopped we decreased the temperature at a rate of 2 K/min from 900 K to room temperature. The resulting electrical resistivity under cooling of the Sr_2FeMoO_6 can be seen in Fig. 1. For a best description of this behavior we separate three regions: (A) from 300 K to 405(10) K where the electrical resistivity has metallic behavior. (B) Above this temperature a change in the sign of the slope can be observed, showing a localization of the electrical carriers up to approximately 590 K and (C) from this temperature to 900 K where the material becomes metallic again. In summary increasing T we observe the sequence metal, semiconductor, and metal, where we can define approximately two metal-insulator transitions at $T_{MI,1}$ and $T_{MI,2}$ at 405 K and 590 K, respectively.

In Fig. 2 we show an experiment at room temperature. We measured the evolution of ρ with time having initially the sample under vacuum, where $\rho\approx\rho_b$. When we broke the vacuum to atmospheric pressure, ρ increases notably with time. We explain this behavior as due to the incorporation of oxygen at the grain boundary, increasing the ρ_{gb}, and affecting the total electrical resistivity $\rho=\rho_{gb}+\rho_b$ The samples measured in air showed semiconducting behavior in the whole temperature range studied and a 4.7% of magnetoresistance at 14 kG at room temperature. This value is similar to the highest ones reported in the literature.[3] It is worth mentioning that the resistivity behavior shown in Figs. 1 and 2 is reversible and reproducible. Due to the high sensitivity of this compound to oxidation, we performed the rest of the experiments under high vacuum or 10% H_2/Ar atmospheres.

B. Magnetic susceptibility

The magnetic characterization of our samples was carried out through several experiments. From the hysteresis loop at 5 K, we take at $H=50$ kG the magnetization value as the saturated magnetization $M_s=35.4$ emu/g (or $2.7\mu_B$/f.u.). This value is similar to that reported by Kobayashi *et al.*[3] [see inset of Fig. 3(a)]. M_s in an ordered ferrimagnetic configuration of Fe^{3+} and Mo^{5+} would be $4\mu_B$/f.u. The low observed M_s values for this material have been recently explained by a Monte Carlo simulation[13] taking into account two mechanisms to reduce the magnetization. One is a partial disorder in the BB' site in the double perovskite $A_2BB'O_6$. This effect reduces the M_s due to the presence of antiferromagnetic Fe-O-Fe and paramagnetic Mo-O-Mo exchange interactions. The second mechanism is associated with the presence of oxygen vacancies that switch off the superexchange interaction between magnetic Fe and Mo cations. Both mechanisms reduce M_s with respect to an ideal material, no oxygen vacancies, and ordered cations.

Magnetization data as a function of temperature [Fig. 3(a)] taken at 5 kG were used to determine the Curie temperature as the minimum value in the dM/dT vs T curve [Fig. 3(b)] given $T_C\simeq405(4)$ K. In Fig. 3(c) we plot H/M taken as the inverse of the magnetic susceptibility, and it is observable that it does not follow a Curie-Weiss law at all. However, as a rough approximation, a Curie-Weiss temperature $\Theta=416(13)$ K was estimated by extrapolation when $H/M=0$ from the linear behavior in a short temperature interval near T_C [solid line in Fig. 3(c)], and it is very close to the Curie temperature. From the slope we obtained an effective magnetic moment $\mu_{eff}=6.7(3)\mu_B$. This value is

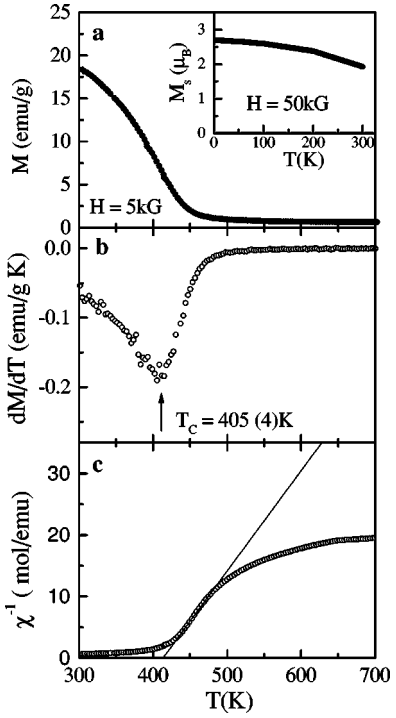

FIG. 3. Temperature dependence of (a) M ($H=5$ kG). The inset shows the saturated magnetization at low T. (b) dM/dT determining the Curie temperature (T_C). (c) Inverse of susceptibility. The straight line shows a fit with a Curie-Weiss law and the determination of the Curie-Weiss temperature ($\Theta=416$ K).

greater than the $\mu=\sqrt{\mu_{Fe}^2+\mu_{Mo}^2}=6.1\mu_B$ expected for one Fe^{3+} ($S=5/2,5.9\mu_B$) and one Mo^{5+} ($S=1/2,1.7\mu_B$) per unit formula. This difference, together with the fact that at higher temperatures the susceptibility tends to be constant, indicates the presence of itinerant electrons adding a constant value to the susceptibility.

C. Electron spin resonance spectroscopy

The ESR line shape for sintered pellets was Dysonian. Lorentzian line shapes were obtained when the ceramic samples were reduced to fine powder and mixed with quartz powder. The ESR spectra for $T\leqslant T_C$ are shown in Fig. 4(a). The shift of the center of the magnetic field and the narrowing of the line with increasing T are clearly observable.

On the other hand, the spectra for $T>T_C$ [Fig. 4(b)] present a constant value of the resonance magnetic field that corresponds to $g=2.009(5)$, indicating the presence of paramagnetic Fe^{3+} ions.[14] It is also easy to observe that the linewidth increases and the intensity quickly decreases with temperature. In Fig. 4(b), three representative spectra in the T_C to 520 K temperature range are plotted.

At high temperatures, between 520 K and 600 K, the intensity of the paramagnetic line decreases notably, and it becomes difficult to obtain the parameters that characterize the resonance line. However, in this region a second resonance can be clearly observed as shown in Fig. 5. It is centered at $g=1.951(1)$, which is close to the paramagnetic Mo^{5+} ions.[15] This line is narrow with a ΔH_{pp} value of $\sim$64 G. No changes with T in ΔH_{pp} were observed; nevertheless, the peak-to-peak height of the line (h_{pp}) has a linear behavior as a function of $1/T$, thus obeying a Curie law.

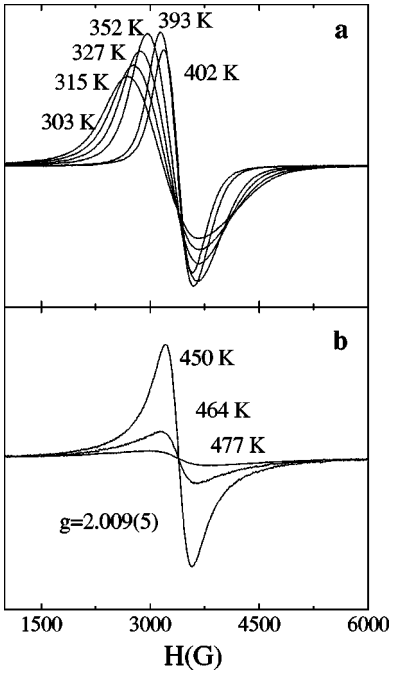

FIG. 4. ESR spectra of Sr_2FeMoO_6 taken at 9.52 GHz. (a) In the region $T<T_C$. (b) In the paramagnetic region $T_C<T<500$ K, where $g=2.009$ corresponds to Fe^{3+} ions.

The temperature dependence of the resonance center field (H_0) is shown in Fig. 6, where we also indicate the magnetic field resonance expected for paramagnetic Fe^{3+} and Mo^{5+} ions. Below T_C, the field H_0 diminishes with decreasing T due to the internal magnetic field coming from the magnetic order of the material. At high T ($\geqslant$520 K), we only plot the H_0 values of the narrow line.

The experimental peak-to-peak linewidth (ΔH_{pp}) for the crystalline powder of Sr_2FeMoO_6 as a function of temperature is presented in Fig. 7. The ΔH_{pp} shows a minimum of $\approx$270 G at $T_{min}\sim 1.05T_C$, which is similar to manganites.[16] Below this temperature $\Delta H_{pp}(T)$ increases with decreasing

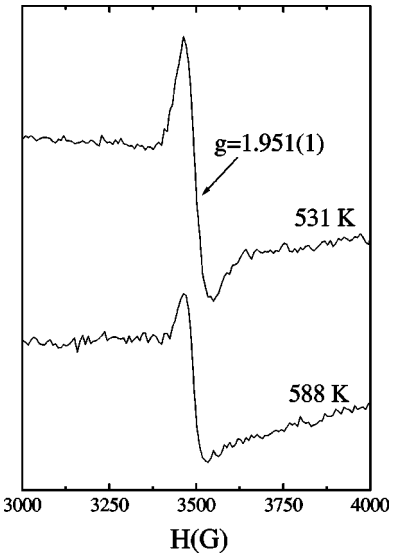

FIG. 5. ESR spectra of Sr_2FeMoO_6 taken at 9.52 GHz in the region $T>500$ K. These resonance lines correspond to paramagnetic Mo^{5+} ions.

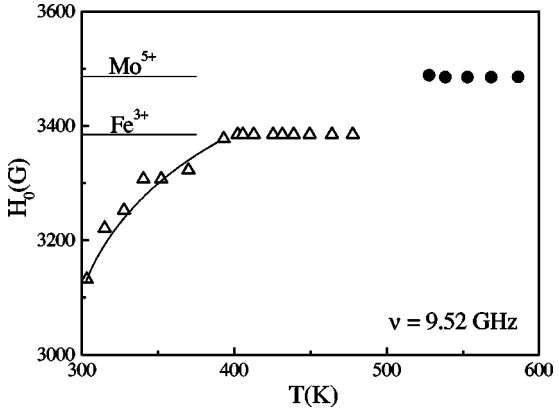

FIG. 6. ESR center field (H_0) of the observed resonance lines of Sr_2FeMoO_6, as a function of temperature. The lines indicate the expected H_0 values for paramagnetic Fe^{3+} and Mo^{5+} ions.

T, reaching values of 1000 G at room temperature ($\sim 0.70 T_{min}$). Above T_{min}, ΔH_{pp} increases with T reaching 1400 G at 520 K.

In Fig. 8 curve B represents the Curie-Weiss law for the Fe^{3+} ions, $\chi_{Fe}(T) = C_{Fe^{3+}}/(T - 416\ \mathrm{K})$. The line intensity $I(T)$ can be computed as a numerical double integration of the resonance line (area under the absorption curve). Corrections by a skin depth effect ($\delta = \sqrt{2\rho/\mu_0\omega}$) that could change the number of resonant ions and by a short magnetic field sweep that could cut the tail of the Lorentzian lines have been taken into account. Both corrections are negligible. The value of the intensity is proportional to the magnetic susceptibility of the resonant ions. Therefore, at 450 K where we observe the Fe^{3+} resonance and the line shape is Lorentzian [see Figs. 4(b) and 6], we multiply the $I(T)$ data by a constant (f) in order to obtain $\chi_{Fe}(450\ \mathrm{K})$. We name ESR susceptibility (χ_{ESR}) to the result of $f \times I(T)$ for the range of T studied and it is plotted as solid circles in Fig. 8. Note the difference between χ_{ESR} and χ_{Fe} at high T. This could indicate that the number of resonant Fe^{3+} ions diminishes with T.

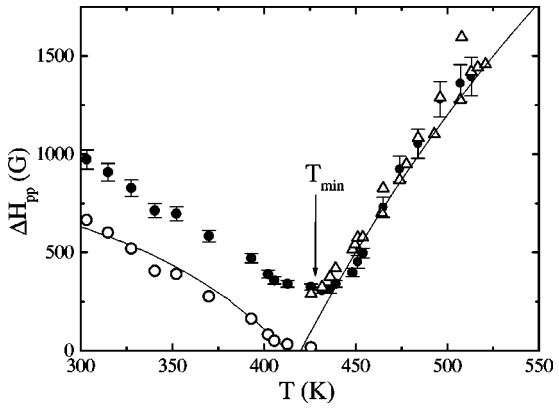

FIG. 7. Experimental peak-to-peak ESR linewidth (solid circles) as a function of temperature. At $T < T_C$, the open circles indicate the excess of the linewidth (see text) and the solid line is the fitting of the data with Eq. (6). At $T > T_C$, the open triangles are the ΔH_{pp} calculated from the χ_{ESR} data with Eq. (7) in the paramagnetic region, taking $\Delta H_{pp}^{\infty} = 7500$ G (see text). The solid line ($T > T_C$) corresponds to $\Delta H_{pp}(T) = [1 - \Theta/T]\Delta H_{pp}^{\infty}$.

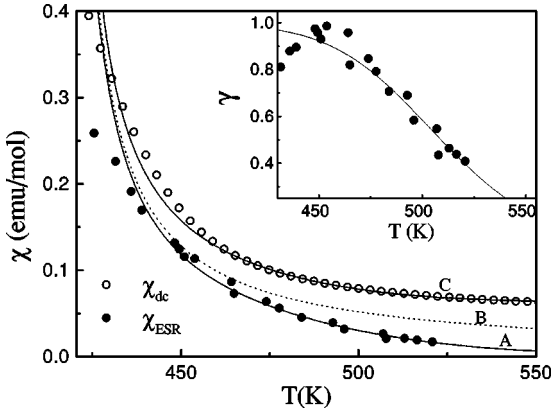

FIG. 8. ESR susceptibility χ_{ESR} (solid circles) and χ_{dc} data (open circles) as a function of temperature. The solid line A is the fit $\chi_{loc} = \gamma(T) C_{Fe^{3+}}/(T - \Theta)$, with $\gamma(T)$ as shown in the inset. The dotted line B is the Curie-Weiss law for the Fe^{3+} ions and curve C is $\chi_{loc} + \chi_{itin}$ (see text).

At $T = 520$ K where the two resonances are observed, we calculated $I(T)$ for each of them as $I(T) = h_{pp}(T)[\Delta Hpp(T)]^2$. From these intensities we can estimate the ratio of Fe to Mo ions as the number $N_{Fe}/N_{Mo} \approx I_{Fe}\mu_{Mo}^2/I_{Mo}\mu_{Fe}^2 \approx 30$. It indicates that only a few Mo ions contribute to the intensity of the resonance line. This ratio is not constant, diminishing with T due to the different temperature dependence of both intensities. The Mo^{5+} resonance line follows a Curie law, while the resonance of Fe^{3+} ions does not show this behavior, as we will see below.

IV. DISCUSSION

We observe an appreciable change in the resistivity of this compound by modification of the oxygen content at the grain boundaries. This instability of the grain boundaries hampers the study of the bulk resistivity. Therefore, in order to study the bulk properties, the experiments were performed under high vacuum or 10% H_2/Ar atmosphere (see Fig. 2). On the other hand, in the samples where the grain boundary effect is present, we measure at $H = 14$ kG and at room temperature a magnetoresistance of 4.7%. In this material the magnetoresistance is mainly due to a grain boundary effect[17] because of the spin polarization of the charge carriers, which is responsible for the half-metallic character of this compound.[3] From the bulk resistivity measurements two metal-insulator transitions at $T_{MI,1} = 405$ K and $T_{MI,2} = 590$ K were found.

Early high-temperature susceptibility measurements[9] showed in a χ^{-1} vs T plot a concave downwards curve. This behavior and the small value of the saturated magnetization extrapolated to 0 K were associated with ferrimagnetism. However, we postulate that the concave downwards $\chi^{-1}(T)$ is due to the metallic character of this compound. The Curie-Weiss (CW) law obtained from the linear portion of the $\chi^{-1}(T)$ vs T curve (see Fig. 3) only applies in a small T range, showing a deviation at high T with respect to the experimental data. Furthermore, the Curie constant obtained is too high as compared to the maximum expected value $C = C_{Fe^{3+}} + C_{Mo^{5+}}$ considering all the spins as localized. In the ESR measurements, the Mo^{5+} ions were practically not observed, and a band calculation[3] shows that the $4d$ elec-

trons of these ions should be partially filling the conduction band. These observations could indicate that these electrons are itinerants. However, the electrical resistivity shows a semiconducting region or localization of the carriers (see Fig. 1). This behavior could be related to a weak Anderson localization[18–20] with an associated gap of ~ 3 meV. This localization should be induced by the same disorder that reduces the saturated magnetization, i.e., some disorder in the Fe and Mo sites, or the presence of oxygen vacancies as was mentioned above. When the T_{MI2} is reached, the Fermi level equals the energy of the mobility edge and the compound becomes metallic again. In a completely ordered perovskite without grain boundary effects it should be metallic in the whole temperature range.

According to this picture, the paramagnetic susceptibility should be

$$\chi = \chi_{loc} + \chi_{itin}, \tag{1}$$

where the first term represents the contribution to the susceptibility of the localized moments and they could present a CW dependence $[\chi = C/(T-\Theta)]$. The second term of Eq. (1) is the metallic contribution and we expect a constant value due to a Pauli (χ_{Pauli}) and Landau (χ_{Landau}) susceptibilities:

$$\chi_{itin} = \chi_{Pauli} + \chi_{Landau}. \tag{2}$$

In this frame, the maximum χ_{loc} is found when the electrons of the Fe^{3+} ions are fully localized; thus $C = C_{Fe^{3+}}$ (see curve B in Fig. 8). However, the experimental values of $\chi_{ESR} = \chi_{loc}$ (solid circles in Fig. 8) decay faster than the CW law. Thus, we think that a temperature-dependent fraction γ of the Fe^{3+} ions have localized spins, in which case $C = \gamma(T) C_{Fe^{3+}}$; then $\gamma(T) = \chi_{ESR}(T-\Theta)/C_{Fe^{3+}}$ as shown in the inset of Fig. 8. Note that near T_C the γ values are close to 1 and decay rapidly with T reaching 0.4 at 520 K. Now, we can suppose that at a given T, the system presents a fraction γ of Fe^{3+} ions with localized spins in equilibrium with a fraction $1-\gamma$ of delocalized ions ($[Fe^{3+}]_{loc} \rightleftharpoons [Fe^{3+}]_{itin}$). This ''reaction'' can be described by an equilibrium constant[21] which follows an Arrhenius law

$$K = \frac{[Fe^{3+}]_{itin}}{[Fe^{3+}]_{loc}} = \frac{1-\gamma}{\gamma} = A \exp\left(-\frac{\Delta}{RT}\right). \tag{3}$$

In this way we obtain

$$\gamma = \frac{1}{1 + A \exp(-\Delta/RT)}. \tag{4}$$

The solid line in the inset of Fig. 8 shows the fit of γ data with Eq. (4) using $A = 1.6 \times 10^8$, $\Delta = 80$ kJ/mol (0.83 eV), and the constant $R = 8.314$ J/(mol K). Curve A in Fig. 8 represents the adjustment $\chi_{loc} = \gamma(T) C_{Fe^{3+}}/(T-\Theta)$. In order to explain the experimental magnetic dc susceptibility, we must add χ_{itin} to χ_{loc} as shown in Eq. (1). However, we have to take into account two contributions to χ_{itin}, one coming from the Mo^{5+} ions (independent of temperature) and the second from delocalized spins of Fe^{3+}, which varies as $1 - \gamma(T)$:

$$\chi_{itin} = \chi_{itin}[Mo^{5+}] + [1-\gamma(T)]\chi_{itin}[Fe^{3+}]. \tag{5}$$

With $\chi_{itin}[Mo^{5+}] \approx 0.037$ emu/mol, $\chi_{itin}[Fe^{3+}] \approx 0.026$ emu/mol, and χ_{loc} obtained before we reproduce the total susceptibility data for $T \geqslant 1.1 T_C$ (curve C in Fig. 8).

The ESR data below T_C show that the temperature behavior of the spectrum has the characteristic of a ferromagnetic or ferrimagnetic resonance: the resonance magnetic field increases with temperature and a narrowing of the linewidth is observed.

In Fig. 7 we plot with open circles the excess of linewidth $[\Delta H_{exc} = \Delta H_{pp}(T) - \Delta H_{pp}(T_{min})]$ for $T < T_{\min}$. This excess can be related to the phenomenological equation[16]

$$\Delta H_{exc}(T < T_{\min}) = 4\pi M_s(T)\Phi, \tag{6}$$

where M_s is the saturated magnetization and Φ is a scaling factor. Following the theory developed by Sparks,[22] $\Phi = (v/V)\beta$, where v is the total pore volume, V is the sample volume, and β is a factor that relates some geometrical parameters. This theory considers the demagnetizing field of a spherical pore at the center of a spherical sample as a source of the inhomogeneous broadening. The solid line in Fig. 7 is the excess linewidth obtained with Eq. (6) using our magnetization data at 5 kG.

At $T \geqslant T_C$ the linewidth increases with temperature. Recently, the ΔH_{pp} behavior in the insulating paramagnetic phase (above $T_{\min}$) of perovskites of Mn has been extensively discussed in a series of papers.[23–25] The temperature dependence of the linewidths has been described considering only spin-spin interactions[26] by the simple formula

$$\Delta H_{pp}(T > T_{\min}) = \left[\frac{\chi_0(T)}{\chi_{ESR}(T)}\right] \Delta H_{pp}^{\infty}, \tag{7}$$

where $\chi_0(T)$ denotes the Curie susceptibility of the free spins that contribute to the resonance, $\chi_{ESR}(T)$ is the measured susceptibility, and the second factor ΔH_{pp}^{∞} should be a temperature-independent constant. It is usually described considering exchange narrowing models and contributions due to anisotropic interactions. The classical dipolar interaction is commonly the source of linewidth broadening but in quasicubic perovskites its contribution to ΔH_{pp}^{∞} could be only of a few gauss.[27]

By using Eq. (7) with $\chi_0 = \gamma C_{Fe^{3+}}/T$, the experimental $\chi_{ESR}(T)$ and $\Delta H_{pp}^{\infty} \approx 7500(500)$ G (open triangles in Fig. 7) we can describe the linewidth in the temperature region $T > T_{min}$. Also we plot with a solid line the law $\Delta H_{pp}(T) = [1 - \Theta/T]\Delta H_{pp}^{\infty}$ with the same values of the parameters. The agreement is due to the cancellation of the $\gamma C_{Fe^{3+}}$ factor in both $\chi_0(T)$ and $\chi_{ESR}(T)$.

V. CONCLUSIONS

In this work we have presented electrical resistivity (ρ), magnetic susceptibility (χ), and electron spin resonance data at high temperature for the Sr_2FeMoO_6 double perovskite. In conclusion, we found in the studied temperature region the following.

(i) Sr_2FeMoO_6 is very sensitive to oxidation and the resistivity is strongly dominated by the carrier scattering at the grain boundaries.

(ii) When the oxygen atoms placed at the grain boundaries are removed, we observed two metal-insulator transitions, being clearly metallic below $T_C = T_{MI,1} = 405$ K and above $T_{MI,2} \sim 590$ K. For intermediate temperatures, the system presents a possible Anderson localization of the carriers with semiconducting behavior.

(iii) In the paramagnetic region, the ESR data show the presence of Fe^{3+} ions.

(iv) The intensity of the Fe^{3+} ESR lines decreases faster than a Curie-Weiss law with increasing T, showing that the number of Fe^{3+} localized spins diminishes.

(v) The behavior of the Fe^{3+} ESR linewidth is well described by inhomogeneous broadening below T_C and by only spin-spin interactions above T_C.

(vi) Very small amounts of localized Mo^{5+} ions have been detected at $T > 500$ K.

(vii) $\chi(T)$ in the paramagnetic phase shows the coexistence of Fe^{3+} localized moments with itinerant electrons coming from Mo^{5+} ions and from an increasing fraction of Fe^{3+} ions with temperature.

In summary, the high-temperature ESR and magnetization data can be explained by a simple model considering all the Mo^{5+} ions with delocalized spins and for the Fe^{3+} ions a fraction γ with localized spins and the rest contributing to the itinerant susceptibility. This fraction is temperature dependent and it is related to an equilibrium constant that follows an Arrhenius law.

ACKNOWLEDGMENTS

This work was supported by CNEA (Argentine Atomic Energy Commission), CONICET (Argentine National Research Council), CEB (Bariloche Electricity Company), Fundación Antorchas, CEE (Commission of the European Communities) through DGXII Contract No. CII *CT92-0087, and ANPCyT, Argentina, Grant No. PICT 3-52-1027. The authors gratefully acknowledge the help of Dr. C. Ramos in the English revision and Dr. M. T. Causa for a critical reading of this manuscript. F.R and L.E.H. wish to thank the Ministerio de Educación y Ciencia (Spain) for financial support.

[1] R. Von Helmholt, J. Wecker, B. Holzapfel, L. Schultz, and K. Samwer, Phys. Rev. Lett. **71**, 2331 (1993).
[2] S. Jin, T.H. Tiefel, M. McCormack, R.A. Fastnacht, R. Ramesh, and L.H. Chen, Science **264**, 413 (1994).
[3] K-I. Kobayashi, T. Kimura, H. Sawada, K. Terakura, and Y. Tokura, Nature (London) **395**, 677 (1998).
[4] T. Manako, M. Izumi, Y. Konishi, K-I Kobayashi, M. Kawasaki, and Y. Tokura, Appl. Phys. Lett. **74**, 2215 (1999).
[5] H.Y. Hwang, S-W. Cheong, N.P. Ong, and B. Batlogg, Phys. Rev. Lett. **77**, 2041 (1996).
[6] K-I. Kobayashi, T. Kimura, Y. Tomioka, H. Sawada, K. Terakura, and Y. Tokura, Phys. Rev. B **59**, 11 159 (1999).
[7] F.K. Patterson, C.W. Moeller, and R. Ward, Inorg. Chem. **2**, 196 (1963).
[8] F.S. Galasso, F.C. Douglas, and R.J. Kasper, J. Chem. Phys. **44**, 1672 (1966).
[9] T. Nakagawa, J. Phys. Soc. Jpn. **24**, 806 (1968).
[10] S. Nakayama, T. Nakagawa, and S. Nomura, J. Phys. Soc. Jpn. **24**, 219 (1968).
[11] B. García Landa, C. Ritter, M.R. Ibarra, J. Blasco, P.A. Algarabel, R. Mahendiran, and J. García, Solid State Commun. **110**, 435 (1999).
[12] J. Rodriguez-Carvajal, computer code FULLPROF, Laboratoire Léon Brillouin (CEA-CNRS), 1998.
[13] A.S. Ogale, S.B. Ogale, R. Ramesh, and T. Venkatesan, Appl. Phys. Lett. **75**, 537 (1999).
[14] R.D. Sánchez, M.T. Causa, and R. Carbonio, J. Magn. Magn. Mater. **140-144**, 2147 (1994).
[15] K.D. Bowers and J. Owen, Rep. Prog. Phys. **18**, 304 (1953).
[16] F. Rivadulla, M.A. López-Quintela, L.E. Hueso, J. Rivas, M.T. Causa, C. Ramos, R.D. Sánchez, and M. Tovar, Phys. Rev. B **60**, 11 922 (1999).
[17] H.Q. Yin, J.-S. Zhou, J.-P. Zhou, R. Dass, J.T. McDevitt, and J.B. Goodenough, Appl. Phys. Lett. **75**, 2812 (1999).
[18] N.F. Mott, *Metal Insulator Transitions* (Taylor & Francis, London, 1990).
[19] R. Allub and B. Alascio, Phys. Rev. B **55**, 14 113 (1997).
[20] R. Allub and B. Alascio, Solid State Commun. **99**, 613 (1996).
[21] B. Mahan, *University Chemistry* (Addison-Wesley, Reading, MA, 1975).
[22] E. Schölmann, J. Phys. Chem. Solids **6**, 242 (1958); M. Sparks, J. Appl. Phys. **36**, 1570 (1965).
[23] M. Tovar, G. Alejandro, A. Butera, A. Caneiro, M.T. Causa, F. Prado, and R.D. Sánchez, Phys. Rev. B **60**, 10 199 (1999).
[24] M.T. Causa, M. Tovar, A. Caneiro, F. Prado, G. Ibañez, C.A. Ramos, A. Butera, B. Alascio, X. Obradors, S. Piñol, F. Rivadulla, C. Vazquez, A. López Quintela, J. Rivas, Y. Tokura, and S.B. Oseroff, Phys. Rev. B **58**, 3233 (1998).
[25] D.L. Huber, G. Alejandro, A. Caneiro, M.T. Causa, F. Prado, M. Tovar, and S.B. Oseroff, Phys. Rev. B **60**, 12 155 (1999).
[26] D.L. Huber, J. Phys. Chem. Solids **32**, 2145 (1971); E. Dormann and V. Jaccarino, Phys. Lett. **48A**, 81 (1974); D.L. Huber and M.S. Seehra, J. Phys. Chem. Solids **36**, 723 (1975).
[27] D.L. Huber, J. Appl. Phys. **83**, 6949 (1998).